Journal of Power Sources 198 (2012) 273–280

Contents lists available at SciVerse ScienceDirect

Journal of Power Sources

journal homepage: www.elsevier.com/locate/jpowsour

A study on time-dependent low temperature power performance of a lithium-ion battery

Hyung-Man Cho[a], Woo-Sung Choi[a], Joo-Young Go[b], Sang-Eun Bae[c], Heon-Cheol Shin[a,*]

[a] School of Materials Science and Engineering, Pusan National University, San30, Jangjeon-dong, Geumjeong-gu, Busan 609-735, Republic of Korea
[b] SB LiMotive, R&D Team, 428-5, Gongse-dong, Giheung-gu, Yongin-si, Gyeonggi-do 446-577, Republic of Korea
[c] Nuclear Chemistry Research Division, Korea Atomic Energy Research Institute, Dukjin-dong 150-1, Yuseong-gu, Daejeon 305-353, Republic of Korea

ARTICLE INFO

Article history:
Received 27 July 2011
Received in revised form
30 September 2011
Accepted 30 September 2011
Available online 5 October 2011

Keywords:
Low temperature
Polarization
Power
Lithium battery
Pulse discharging

ABSTRACT

Time-dependent elementary polarizations of a lithium-ion battery are quantitatively investigated below room temperature in an attempt to determine the critical factors affecting low temperature power decline. From three-electrode impedance measurements and the theoretical analysis of the phenomenological equivalent circuit, the proportional contribution of the internal resistances to the total polarization is satisfactorily analyzed as a function of the pulse discharging time. The results prove that the interfacial charge-transfer resistances of the anode (graphite) and the cathode (lithium cobalt dioxide) make the highest contributions to the low temperature power decline. On this basis, a strategy for the material design to enhance the low temperature performance is suggested with two examples of surface modification and hybridization with an electrochemical capacitor.

1. Introduction

Lithium-ion batteries (LIBs) have been used for energy sources in various mobile and fixed applications due to their superior performance compared to other electrochemical energy storage devices [1]. The world-wide energy crisis and air pollution have caused the recent strong demand for high-power LIBs suitable for transportation systems, such as (hybrid) electric vehicles and aircrafts [2–6]. In particular, low temperature (LT) power performance of batteries (*e.g.*, cold cranking amps) is very tricky, so there has been much effort focused on identifying its key controlling factors.

Nevertheless, the clear understanding of the power decline during the LT operation has not been achieved: the time-dependent contribution of the internal cell resistances to cell power is not fully understood over the course of cell operation, which is of great importance for designing a cell that meets power specification requirements for specific transportation systems. For example, in the case of typical urban driving, when short-time acceleration and regenerative braking are frequently repeated, cell design must be focused on reducing the elementary resistances that critically affect the polarization during the initial stage (less than a few seconds) of cell operation. On the contrary, when rural/highway driving is the predominant driving condition, the cell engineer should widen his attention span to the resistive elements influencing power performance over a prolonged operation time.

Modelling the battery operation might be used effectively to estimate the time-dependent polarizations arising from the elementary internal cell resistances. Mathematical models which describe Li-ion transport through the sandwich of cathode, separator, and anode [7–13], and the equivalent circuit models based on the ac impedance spectroscopy [14–18] are well-known theoretical descriptions of LIB operation. The mathematical transport models are quite rigorous but they require many theoretical parameters that are not easily obtainable and need many computational resources. In comparison, the parameters in the equivalent circuit models are easy to be determined and the calculation procedure is quite simple as well.

In previous articles [19–22], the elementary resistances involved in cell operation were successfully differentiated and their proportional time-dependent contributions to the total polarization were quantified for the first time. In addition, this proved that the half-cell test by using a two-electrode cell configuration possibly leads to unreliable results due to disturbance from the signal of the lithium metal counter electrode.

This work provides a further step towards analyzing the time-dependent LT power decline of LIB. The elementary and total polarizations will be systematically analyzed at different current drains as a function of the pulse discharging time, using a full cell of a graphite anode and a $LiCoO_2$ cathode. Especially, the time-dependent contributions of all the resistive elements in both

* Corresponding author. Tel.: +82 51 510 3099; fax: +82 51 512 0528.
E-mail address: hcshin@pusan.ac.kr (H.-C. Shin).

0378-7753/$ – see front matter © 2011 Elsevier B.V. All rights reserved.
doi:10.1016/j.jpowsour.2011.09.111

electrodes to the total polarization will be estimated from the combination of the three-electrode electrochemical measurements and the equivalent circuit analysis, and then a strategy of the electrode design to improve the power density at a low temperature will be discussed. Furthermore, the significant improvement of LT power performance of the cells consisting of hypothetically surface modified materials and an electrode hybridized with an electrochemical capacitor will be demonstrated on the basis of the suggested method.

2. Experimental procedure

A three-electrode cell configuration was employed for the electrochemical measurements. Lithium cobalt dioxide ($LiCoO_2$, Aldrich) and graphite (OCI Materials Co., Ltd., Republic of Korea) were used as the active materials of the cathode and the anode, respectively. The cathode composite ($LiCoO_2$:carbon black:polyvinylidene fluoride (PVdF) = 90:5:5 in weight) was prepared on Al foil while the anode composite (graphite:PVdF = 90:10) was coated on Cu foil. The area and thickness of the resulting cathode composite were about 1.54×10^{-4} m^2 ($\phi = 1.4 \times 10^{-2}$ m) and 85 μm, respectively, and those of the anode composite were about 2.01×10^{-4} m^2 ($\phi = 1.6 \times 10^{-2}$ m) and 34 μm. The masses of $LiCoO_2$ and graphite in each composite were 17.5 and 9.1 mg. The capacity ratio of the anode (negative) to the cathode (positive), *i.e.*, N/P ratio was set to 1.5 in order to avoid undesirable lithium plating on the graphite surface in the course of the LT operation of the cell.

For the reference electrode, the end tip of the Teflon-coated Cu wire (ϕ(Teflon) = 4.5×10^{-4} m; ϕ(Cu) = 1.27×10^{-4} m) was removed and placed between two separators (Celgard 2400). Details on the cell configuration can be found in our previous articles [20–22]. Before the electrochemical experiments, elemental Li was cathodically coated on the bare Cu wire by using a $LiCoO_2$ composite electrode as the counter electrode. For this coating process, a constant current of 0.2 mA was applied for 3 s and then interrupted for 7 s, and this process was repeated dozens of times. The electrolyte was a 1 M solution of lithium hexafluorophosphate ($LiPF_6$) in a 1:1 volume mixture of ethylene carbonate (EC) and diethyl carbonate (DEC). The cell was assembled and hermetically sealed in a glove box (MBraun, Germany) filled with purified argon gas.

The as-prepared cell was first cycled three times between 2.55 and 3.95 V (*vs.* graphite) at a rate of 0.2 C and 25 °C (22 mA per 1 g of $LiCoO_2$; a nominal specific capacity of 110 mAh per 1 g of $LiCoO_2$ was assumed to convert the current density into the C rate). Then, the impedance spectra were obtained over the frequency range of 50 kHz to 5 mHz at a cell potential of 3.95 V (*vs.* graphite) where the potentials of $LiCoO_2$ cathode and graphite anode were about 4.08 and 0.13 V (*vs.* Li/Li^+), respectively. After the impedance measurement, the temperature was changed to 15, 5, or −5 °C at the open circuit condition and the impedance spectra were subsequently obtained at each temperature. The change in the potentials of cathode and anode with temperature was quite trivial. For the tests at different temperatures, controlled temperature chamber was used. The hermetically sealed electrochemical cell was operated inside the chamber.

A pulse discharge test was performed at each temperature right after the impedance measurement: the cell was equilibrated at a constant potential of 3.95 V (*vs.* graphite) and subsequently discharged for 10 s at the cut-off voltage of 2.55 V (*vs.* graphite) over a rate range of 0.2–21 C (2.31 A per 1 g of $LiCoO_2$). Only one cell is used throughout the tests. After each pulse discharging the cell was recharged to the initial potential of 3.95 V (*vs.* graphite) by applying constant current of 0.2 C and then constant potential of 3.95 V (*vs.* graphite). A Solartron 1287 electrochemical interface system was employed to carry out all of the galvanostatic tests. For the electrochemical impedance measurement, the Solartron 1287 system was coupled with a Solartron 1455A frequency response analyzer.

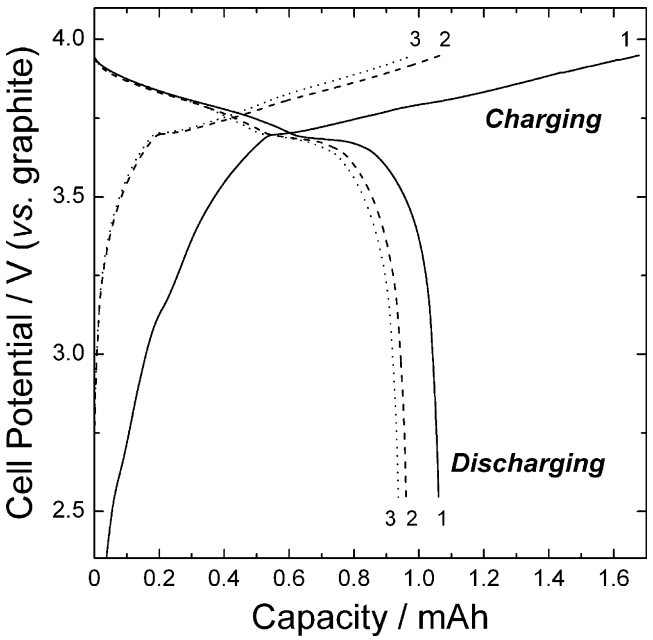

Fig. 1. Voltage profiles of the $LiCoO_2$/graphite cell for the first three cycles at a rate of 0.2 C.

3. Results and discussion

3.1. Diagnosis of low temperature power decline

The voltage profiles of the as-prepared cell for the first three cycles are presented in Fig. 1. Less than 70% of the charge transferred in the first charging process returned in the following discharging process. It is well known that the formation of the solid electrolyte interface (SEI) layer on the graphite leads to such an initial irreversibility. The relatively large irreversible capacity is most likely attributed to the high N/P ratio of the cell. The cell exhibited an excellent reversibility for subsequent cycles and the voltage profile was consistent with that reported previously [23].

The cell potential (or cathodic polarization) transients for 10 s at different discharging rates over the temperature range of −5 to 25 °C are given in Fig. 2. The transients dropped more rapidly as the operating temperature was reduced, which is indicative of the elevated cell polarization and the lowered power density: the cell potential at 25 °C remained above the low cut-off voltage of 2.55 V (*vs.* graphite) throughout the whole discharging process even at the very high rate of 21 C (Fig. 2(a)). Whereas, the potential transients at 15, 5, and −5 °C reached the cut-off voltage before 10 s at much lower discharging rates (Fig. 2(b)). In order to explore the decisive resistive factors in such a LT power decline, an attempt was made to separate the resistive elements involved in the discharging process and then to quantify their contributions to the total cell polarization.

The differentiation of the resistive elements was done both for the cathode and the anode by using electrochemical impedance spectroscopy, as presented in Fig. 3(a) and (b), respectively. All the impedance spectra were characterized by two semicircles and an inclined line. It is generally agreed that the first semicircle relates to either the presence of the SEI layer or the particle-to-particle contact of the active materials while the second semicircle is ascribed to the interfacial charge transfer combined with the double layer

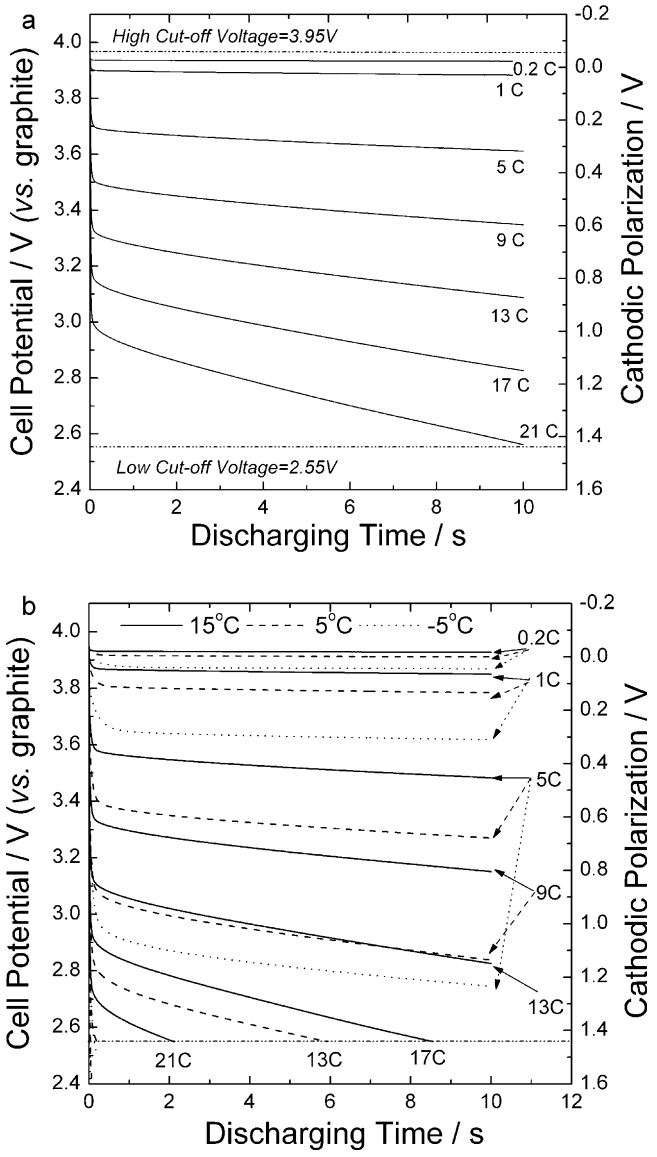

Fig. 2. Cell potential (or total cathodic polarization) transients during the pulse discharging for 10 s, measured from the $LiCoO_2$/graphite cell at different discharging rates and at temperatures of (a) 25 and (b) 15, 5, −5 °C.

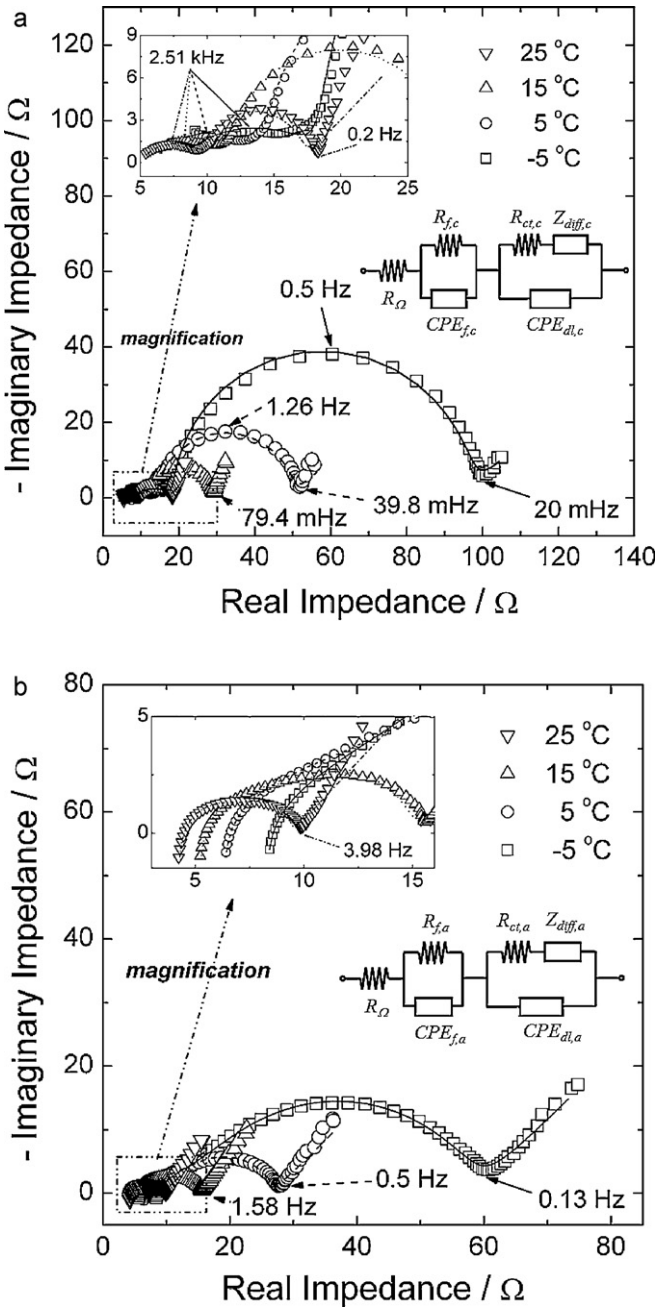

Fig. 3. Impedance spectra of (a) the $LiCoO_2$ and (b) the graphite at a cell potential of 3.95 V (*vs.* graphite) and different temperatures. The potentials of $LiCoO_2$ cathode and graphite anode were about 4.08 and 0.13 V (*vs.* Li/Li^+), respectively, and the change in their values with temperature was quite trivial. The solid and dotted lines were determined from the CNLS fittings of the impedance spectra to the equivalent circuits presented in the insets. R_Ω, R_f and R_{ct} mean the uncompensated ohmic resistance, SEI film (or particle-to-particle contact) resistance and charge transfer resistance. *CPE* and Z_{diff} are the constant phase element and the Warburg impedance, respectively.

charging/discharging process [24,25]. Also, the solid-state lithium diffusion through the active materials is responsible for an inclined line known as the Warburg impedance. The summation of the impedance spectra from the cathode and the anode, *i.e.*, the calculated full cell impedance spectra, quantitatively coincided at all operating temperatures with the full cell spectra measured by using a two-electrode cell configuration (the results are not presented in this work), just like our previous reports [20–22]. This indicates that our three-electrode cell works properly.

It should be mentioned that the cell design with relatively high N/P ratio (1.5) used in this work leads to the smaller resistance of graphite anode due to the increased surface area, as compared to the resistance in the cell design with typical N/P ratio (∼1.0). In other words, the resistance of the first semicircle for graphite was severely under-estimated in this work because of high N/P ratio. On the other hand, the redox potential of the electrode materials at a specific state of charge is affected by the temperature and thereby the amount of Li in the electrode material and charge transfer resistance are changed when the potential is fixed and the temperature is changed. However, in this work, after the impedance spectra were obtained at a cell potential of 3.95 V (*vs.* graphite), the temperature was changed to 15, 5, or −5 °C at the open circuit condition, not at fixed potential. In doing so, it is expected that the amount of Li in the electrode material is not changed when the temperature changes.

The simplified equivalent circuits presented in the insets of Fig. 3 were used for the quantitative analysis of the impedance spectra. The circuit parameters estimated from the CNLS (complex non-linear least squares) fitting method are summarized in

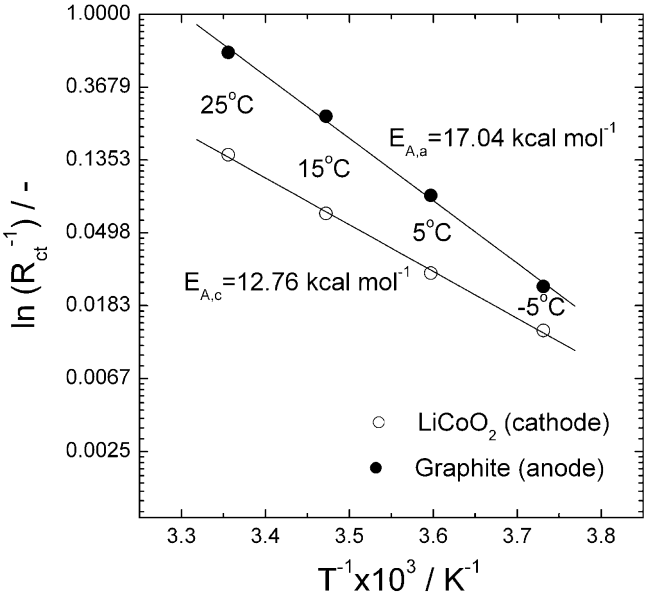

Fig. 4. Arrhenius plots of the charge transfer resistances of the $LiCoO_2$ and the graphite.

Table 1. It is noted that the charge transfer resistances of the $LiCoO_2$ and the graphite were much more sensitive to the operating temperature, as compared to their SEI film resistances (or particle-to-particle contact resistances) and diffusion resistances. Furthermore, although the absolute values of the charge transfer resistance of the $LiCoO_2$ were higher at every temperature than those of the graphite, the Arrhenius analysis proved that the activation energy of the charge transfer reaction on the graphite was even higher than on the $LiCoO_2$ (Fig. 4).

In order to estimate the time-dependent contributions of the elementary resistances to the total cell polarization at different temperatures, the equivalent circuit was re-constructed towards the circuit simulation, as depicted in Fig. 5. In the re-constructed circuit, the Warburg impedance was expressed by an RC transmission line and all of the constant phase elements (CPEs) were considered purely capacitive for the sake of simplicity, as explained in our previous articles [21,22]. On this basis, the total and elementary polarizations were calculated as a function of the discharging time by applying a square current pulse to the circuit.

There might be a concern about the validity of this approach because the circuit parameters might vary within the polarization range of the experiments. Moreover, the change in lithium content on the surface during the pulse discharging process and the concentration polarization in the electrolyte might additionally lower the cell potential. Such three factors possibly lead to the difference between the experimental and calculated polarization transients. Nevertheless, the discrepancy caused by disregarding these factors is thought to be tolerable at the moderate pulse discharging rates where their effects on the cell potential change might be considered relatively small (for further discussion about the effect of circuit parameters, surface potential, and concentration polarization on the cell potential, please see the "Conclusions" in our previous work [21]). In other words, in spite of the small sacrifice of accuracy to gain simplicity, our approach is still quite useful *esp.* at moderate discharging rates, because it provides the fastest and most straightforward way ever reported to evaluate the time-dependent elementary polarizations.

The calculated polarization transients at 25 and −5 °C are given in Fig. 6(a) and (b), respectively, during the cathodic pulse discharging for 10 s at a rate of 5 C. Then, the time-dependent contribution of the elementary resistances to the total polarization was obtained

Table 1
Electrical parameters of (a) $LiCoO_2$ cathode and (b) graphite anode, determined from the complex non-linear least squares (CNLS) fitting of the impedance spectra to the equivalent circuits presented in the insets of Fig. 3.

Temp. (°C)	R_Ω (Ω)	R_f (Ω)	CPE_f[a]		R_{ct} (Ω)	CPE_{dl}[a]		A_ω[b] (Ω s$^{-0.5}$)	D^c (×10^{-11} m^2 s^{-1})	L^d (μm)	$R_D{}^e$ (Ω)	$C_D{}^e$ (F)	r^e (×10^6 Ω m^{-1})	c^e (×10^6 s Ω m^{-1})	Chi-squared (×10^{-3})
			C (mF × s$^{\eta-1}$)	η		C (mF s$^{\eta-1}$)	η								
(a) Cathode ($LiCoO_2$ composite)															
25	4.96	5.18	0.499	0.61	6.88	2.97	1.00	1.55	5.867	5.0	1.0118	0.4211	0.2024	0.08423	6.9499
15	5.12	7.08	1.188	0.50	15.4	3.37	1.00	1.59	5.585	5.0	1.0638	0.4208	0.2128	0.08416	3.0334
5	6.14	8.68	1.119	0.50	34.9	3.67	0.98	1.70	5.216	5.0	1.1769	0.4072	0.2354	0.08145	1.9897
−5	7.54	11.6	0.971	0.50	76.6	3.69	1.00	2.21	4.981	5.0	1.5657	0.3206	0.3131	0.06411	3.7218
(b) Anode (graphite composite)															
25	4.10	3.64	0.231	0.73	1.69	0.438	0.99	1.64	0.854	18	10.102	3.7558	0.5612	0.2087	5.8431
15	4.99	5.92	0.498	0.65	4.05	0.765	0.93	1.99	0.845	18	12.322	3.1117	0.6846	0.1729	0.8875
5	6.01	8.77	0.962	0.58	12.0	0.991	0.84	2.48	0.834	18	15.458	2.5133	0.8588	0.1396	1.0380
−5	7.95	8.96	1.030	0.57	41.9	1.021	0.74	3.68	0.825	18	23.062	1.7029	1.2812	0.0946	0.2556

[a] *CPE* was expressed in the form of $C(j\omega)^\eta$ ($0.5 < \eta \leq 1$).
[b] A_ω is the Warburg coefficient found in the equation of $Z_{diff} = A_\omega(j\omega)^{-0.5}\tanh[\delta(j\omega)^{0.5}]$ (where δ is defined as $L/D^{0.5}$).
[c] Chemical diffusion coefficient D at 3.95 V (*vs.* graphite) was estimated from the galvanostatic intermittent titration technique [26].
[d] Solid state diffusion length L was roughly estimated to be the radius of particle from the microscopic observation.
[e] $R_D = A_\omega L D^{-0.5}$, $C_D = L^2 R_D^{-1} D^{-1}$, $r = R_D L^{-1}$, and $c = C_D L^{-1}$ (where R_D and C_D are the diffusion resistance and capacitance, respectively).

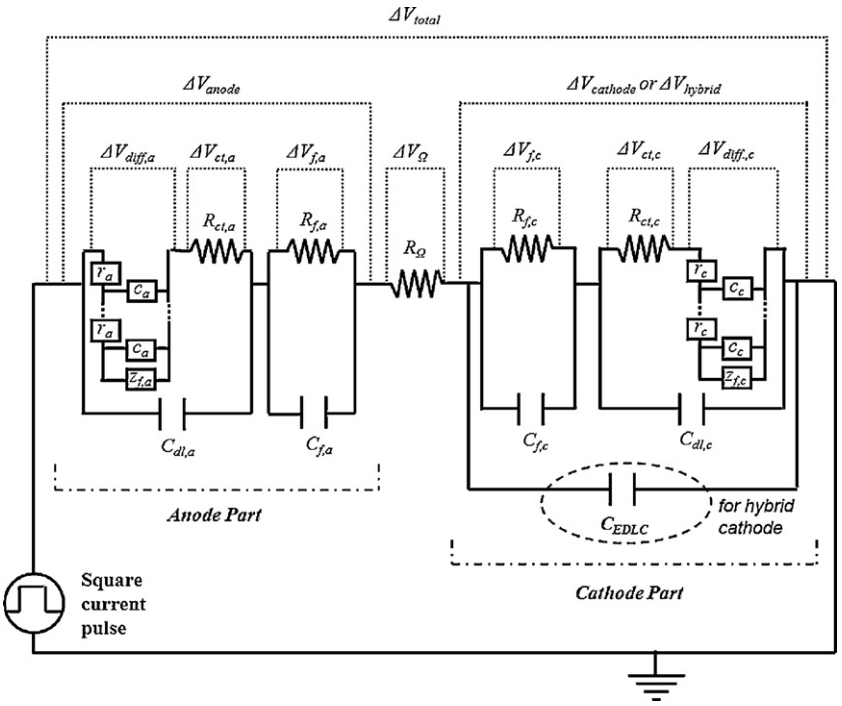

Fig. 5. Equivalent circuit used for the theoretical analysis of the pulse discharge behavior of the $LiCoO_2$/graphite cell. ΔV_{Ω}, ΔV_f, ΔV_{ct}, ΔV_{diff}, and ΔV_{total} represent the polarizations due to the uncompensated ohmic resistance, SEI film (or particle-to-particle contact) resistance, charge transfer resistance, diffusion resistance, and total cell resistance, respectively. For the circuit simulation, the Warburg impedance Z_{diff} was modelled by an RC transmission line, consisting of the elemental resistance (r), the elemental capacitance (c), and the termination load of the infinite impedance for ion transport (Z_f).

from there, as presented in Fig. 7. Since $p(\Delta V)$ in the figure gives an information about how much a specific polarization contributes to the total polarization, one can make a rapid diagnosis of decisive factors affecting cell power as a function of time.

It is noted that the activation polarizations of the $LiCoO_2$ and the graphite, $\Delta V_{ct,c}$ and $\Delta V_{ct,a}$, respectively, increased significantly as the operating temperature decreased from 25 to −5 °C (Fig. 6). As a result, they became the two major sources responsible for the LT power decline (Fig. 7(b)). It is additionally noteworthy that the contribution of the diffusion impedances of the $LiCoO_2$ and the graphite to the total polarization (*i.e.*, $p(\Delta V_{diff,c})$ and $p(\Delta V_{diff,a})$ in Fig. 7) decreased considerably as the operating temperature decreased. Specifically, their contributions fell to less than 10% at −5 °C and became trivial, as compared to the charge transfer resistances.

3.2. Improvement of low temperature power performance

The results in the previous part strongly indicate that the reduction of the reaction barrier for the interfacial charge transfer must come first to enhance the LT power performance. One of the most promising options might be the surface modification of the active materials, which possibly provides a viable way to decrease the activation energy of the charge transfer reaction. The other is an expedient method to minimize the degree of the Faradaic reaction at the interface during the pulse discharging process by hybridizing with a non-Faradaic reaction source, like an electrical double layer capacitor (EDLC). The effect of the surface modification and the hybridization with an EDLC on the LT power performance is hypothetically considered next on the basis of the aforementioned method.

3.2.1. Surface modification

Much effort has been made in recent years to improve the battery performance with surface modifications [27–32]. Among these, the work by Mancini et al. is particularly noteworthy [31]. They found that the activation energy of the charge transfer reaction on the pristine partially oxidized graphite decreased by about 13% (from 13.6 to 11.9 kcal mol^{-1}) due to coating the graphite surface with a few-nanometer thick Cu layers. A decrease in the activation energy results in a lowered susceptibility to temperature. Thus, the charge transfer resistance of the surface modified graphite is expected to be smaller than that of unmodified one *esp.* at low temperatures and its difference between two samples becomes larger as the operating temperature decreases.

Under the circumstances, it will be quite interesting to investigate how much the reduction in the activation energy for charge transfer reaction affects the time-dependent polarization during the pulse discharging. For this purpose, we assumed that the activation energies for the charge transfer reactions on both the $LiCoO_2$ and graphite decreased by the same percentage as in the work by Mancini et al. [31] (*i.e.*, from 12.76 (17.04) to 11.10 (14.82) kcal mol^{-1} for $LiCoO_2$ (graphite)) due to the surface modification and yet the charge transfer resistances at 25 °C remained unchanged. This assumption forces the low-temperature charge transfer resistance of the hypothetically coated materials to be smaller than that of the pristine ones and provides a rough-and-ready model for the study on the effect of activation energy on low-temperature time-dependent polarization.

The charge transfer resistances of the hypothetical, surface-coated $LiCoO_2$ and graphite were estimated from the Arrhenius relation and the time-dependent polarizations were calculated at −5 °C and at a rate of 5 C. The activation polarizations, $\Delta V_{ct,c}$ and $\Delta V_{ct,a}$, of the hypothetical $LiCoO_2$ and graphite, respectively, are shown as a function of the pulse discharging time in Fig. 8(a), together with the corresponding polarization transients of the original, pristine materials. It is noted that $\Delta V_{ct,c}$ and $\Delta V_{ct,a}$ decreased by half after the surface modification. Such a reduction in the activation polarizations significantly influences the total polarization value: ΔV_{total} at 10 s decreased by 0.3 V from 1.33 to 1.03 V at a rate of 5 C by virtue of the surface modification and the cell was

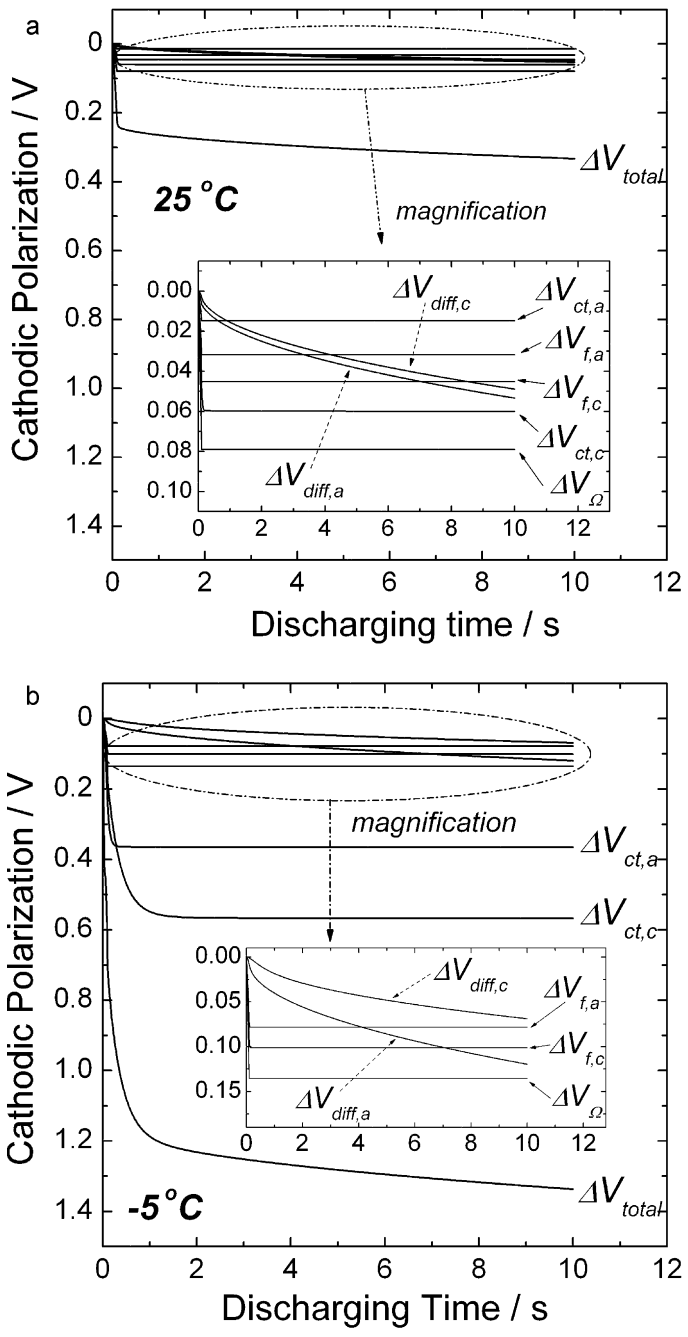

Fig. 6. Variations of the elementary and total polarizations with discharging time at a rate of 5 C and temperatures of (a) 25 and (b) −5 °C.

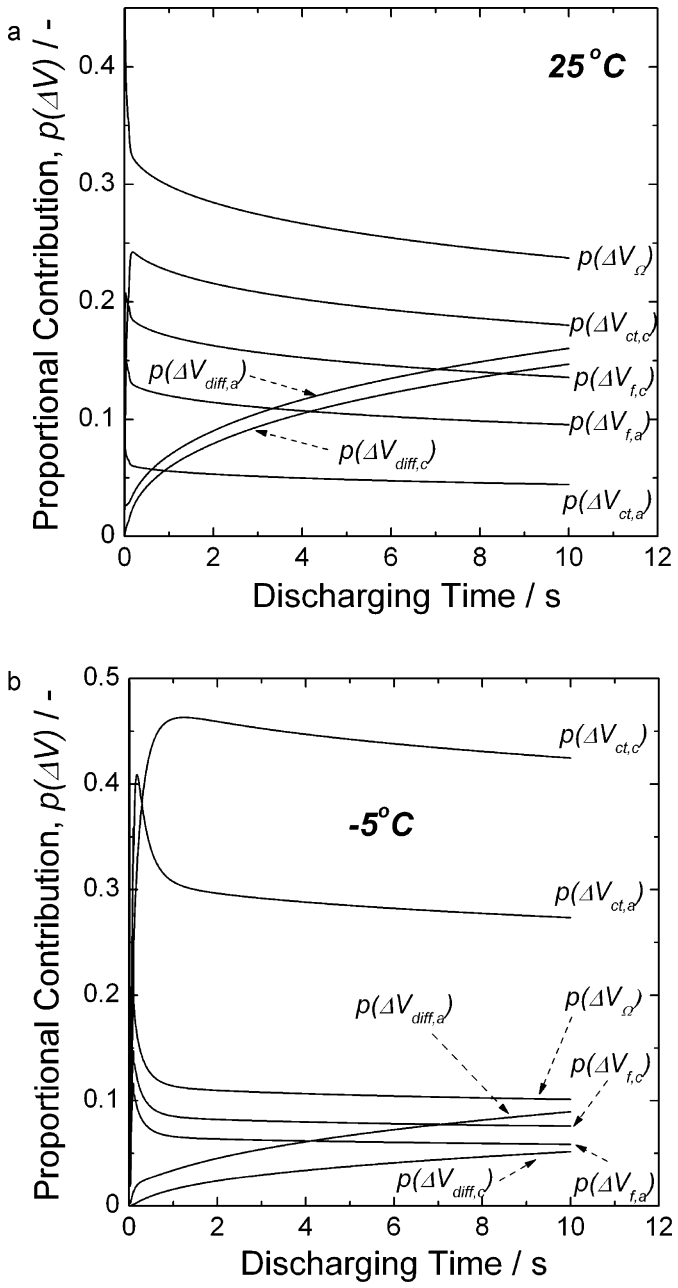

Fig. 7. Time-dependent proportional contributions of the elementary resistances to the total polarization at temperatures of (a) 25 and (b) −5 °C.

accordingly capable of discharging at the higher rate of *ca.* 7 C, as demonstrated in Fig. 8(b).

Nevertheless, it should be mentioned that the experimental realization of the decreased charge transfer resistance of the non-oxidized graphite and $LiCoO_2$ used in this work by surface modifications is still a great challenge. Much work needs to be done to reduce the activation energy by proper surface modifications.

3.2.2. Hybrid electrode

Hybrid cells have attracted much recent attention for their potential applications to high rate energy storage. A case in point is the asymmetric hybrid cell of an activated carbon cathode and an intercalation compound anode, typically used in nonaqueous EDLC and LIB, respectively [33–35]. Although it has been reported that such an asymmetric hybrid cell exhibited an excellent LT performance and fast recharge capability, the electrode operated under either the typical battery working concept or the capacitor working concept still has its inherent drawbacks. In other words, the power performance of the above hybrid cell should basically be limited by the anode side including the intercalation compounds.

In order to resolve this problem, the integration of the intercalation compound and capacitor material into one electrode might deserve consideration [34,36,37]. Apart from the selection of the capacitor material compatible to the specific intercalation compound and relevant electrolyte chemistry, the integrated or hybrid electrode is an intriguing conceptual option because it possibly has both the advantages of intercalation compound and capacitor material. Since it was shown that the resistance for the charge transfer reaction on the cathode made the highest contribution to the LT cell polarization in this work, the hybrid

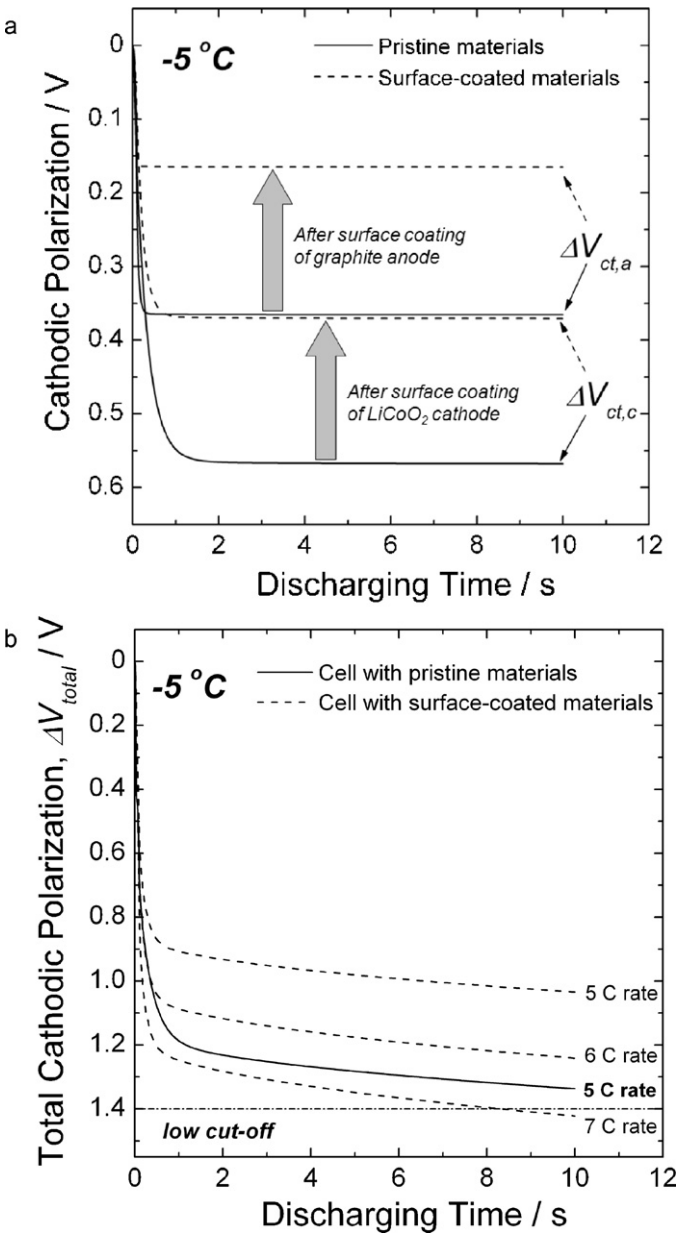

Fig. 8. (a) Cathodic polarization transients at a discharging rate of 5 C and a temperature of −5 °C, due to the charge transfer resistances of the pristine and surface-coated samples of $LiCoO_2$ and graphite, and (b) the corresponding total cathodic polarization transients.

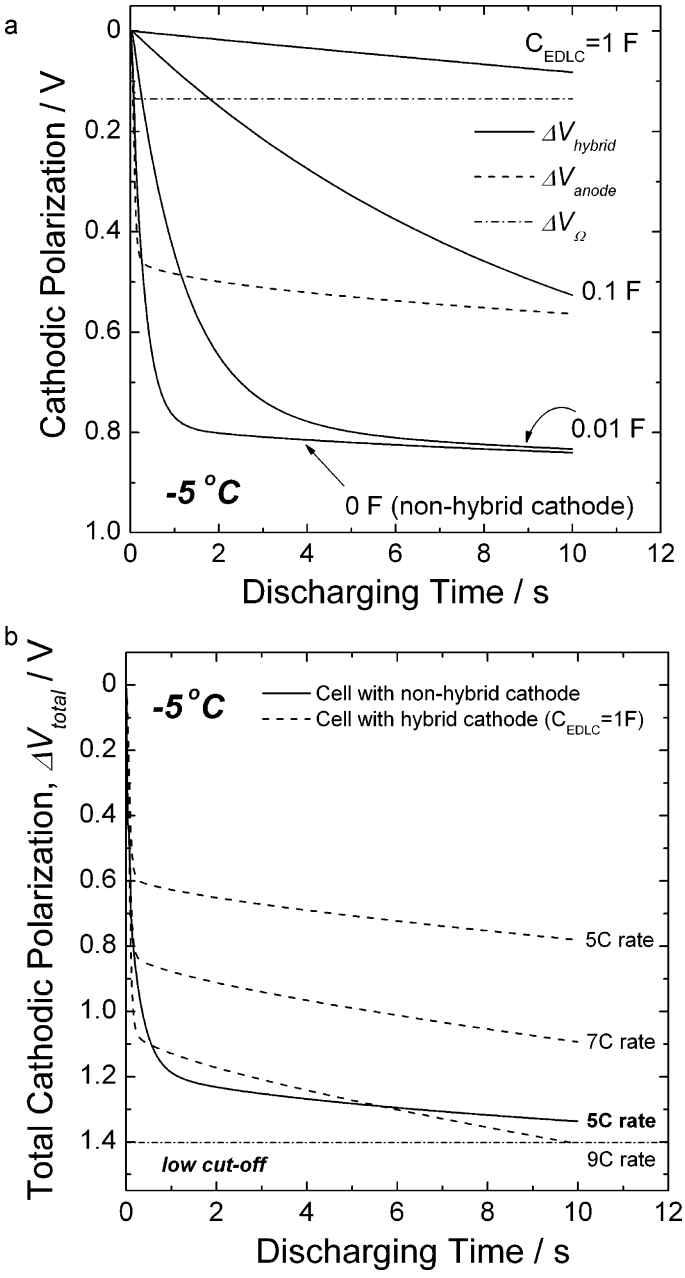

Fig. 9. (a) Cathodic polarization transients at a discharging rate of 5 C and a temperature of −5 °C, calculated for the hybrid cathode composed of the $LiCoO_2$ and the hypothetical EDLC material with different capacitance values. Polarization transients for the graphite anode and the electrolyte were included in the figure. (b) Total cathodic polarization transients of the cells with the non-hybrid and hybrid cathodes.

cathode composed of the $LiCoO_2$ and the hypothetical EDLC material might be a possible solution for the LT power decline.

The reaction of the hybrid cathode is modelled by the parallel combination of the capacitor for the EDLC reaction with the electrical elements for the $LiCoO_2$ reaction (see the cathode part in Fig. 5), because an EDLC stores or dissipates the charge independent of an insertion material. Based on an equivalent circuit for the cell including the hybrid cathode, the time-dependent cathodic polarization was calculated at −5 °C and at a rate of 5 C as a function of the EDLC capacitance. It is noted that the increased EDLC capacitance leads to a milder increase with time in the polarization of the hybrid cathode, as presented in Fig. 9(a).

As a rough calculation for better understanding, assuming the anion (PF_6^-) double-layer capacitance of the activated carbon is 100 F g^{-1} [33,36], 10 mg of the activated carbon is needed for 1 F of capacitance. Thus, the portion of the activated carbon in the hybrid cathode would be about one third of the total active mass (activated carbon + $LiCoO_2$) in this work. When the EDLC capacitance was raised from 0 to 1 F, the polarization of the hybrid cathode at 10 s was significantly dropped from 0.83 to 0.07 V (Fig. 9(a)). As a result, the cell with the hybrid cathode could be continuously discharged for 10 s at a much higher rate of 9 C, as compared to the maximum discharging rate (5 C) of the cell with the non-hybrid cathode (Fig. 9(b)). Since the hybrid electrode concept appears to be very promising based on the calculated results, it would be very meaningful to prepare the hybrid electrode and to make experimental tests to prove the concept. This work is in progress and the results will be reported in a separate paper.

4. Conclusions

In this work, the critical factors affecting the LT power decline of an LIB were systematically investigated from the combination of the three-electrode impedance measurements and the equivalent circuit simulation. The quantitative analysis on the relative contribution of the elementary polarizations proved that the interfacial charge-transfer resistances of the graphite anode and the $LiCoO_2$ cathode were two major sources of the LT cell polarization during the pulse discharging process. The hypothetical demonstrations showed that the decrease in the activation energy for the charge transfer reaction due to the surface modification and the parallel combination of the Faradaic and non-Faradaic mechanisms by the use of hybridizing insertion materials with an electrochemical capacitor might significantly enhance LT performance.

Acknowledgements

This work was supported by the Converging Research Center Program through the Ministry of Education, Science and Technology (2011K000640). Furthermore, this work was partially supported by the NCRC (National Core Research Center) program through the National Research Foundation of Korea funded by the Ministry of Education, Science and Technology (2010-0001-226).

References

[1] M.S. Whittingham, Chem. Rev. 104 (2004) 4271.
[2] A.N. Jansen, A.J. Kahaian, K.D. Kepler, P.A. Nelson, K. Amine, D.W. Dees, D.R. Vissers, M.M. Thackeray, J. Power Sources 81 (1999) 902.
[3] C. Fellner, J. Newman, J. Power Sources 85 (2000) 229.
[4] T. Horiba, T. Maeshima, T. Matsumura, M. Koseki, J. Arai, Y. Muranaka, J. Power Sources 146 (2005) 107.
[5] M.W. Verbrugge, R.Y. Ying, J. Electrochem. Soc. 154 (2007) A949.
[6] FreedomCAR Battery Test Manual for Power-Assist Hybrid Electric Vehicles, Idaho National Engineering & Environmental Laboratory, Department of Energy, DOE/ID-11069, October 2003.
[7] T.F. Fuller, M. Doyle, J. Newman, J. Electrochem. Soc. 141 (1994) 1.
[8] I.J. Ong, J. Newman, J. Electrochem. Soc. 146 (1999) 4360.
[9] P. Arora, M. Doyle, A.S. Gozdz, R.E. White, J. Newman, J. Power Sources 88 (2000) 219.
[10] M. Doyle, Y. Fuentes, J. Electrochem. Soc. 150 (2003) A706.
[11] K. Smith, C.-Y. Wang, J. Power Sources 161 (2006) 628.
[12] K. Kumaresan, G. Sikha, R.E. White, J. Electrochem. Soc. 155 (2008) A164.
[13] D.M. Bernardi, J.-Y. Go, J. Power Sources 196 (2011) 412.
[14] S. Abu-Sharkh, D. Doerffel, J. Power Sources 130 (2004) 266.
[15] B.Y. Liaw, G. Nagasubramanian, R.G. Jungst, D.H. Doughty, Solid State Ionics 175 (2004) 835.
[16] S. Buller, M. Thele, R.W. De doncker, E. Karden, IEEE Trans. Ind. Appl. 41 (2005) 742.
[17] M.W. Verbrugge, P. Liu, J. Power Sources 174 (2007) 2.
[18] Y. Hu, S. Yurkovich, Y. Guezennec, B.J. Yurkovich, Control Eng. Practice 17 (2009) 1190.
[19] D.-K. Kang, H.-C. Shin, J. Solid State Electrochem. 11 (2007) 1405.
[20] H.-M. Cho, Y.J. Park, J.-W. Yeon, H.-C. Shin, Electron. Mater. Lett. 5 (2009) 169.
[21] H.-M. Cho, Y.J. Park, H.-C. Shin, J. Electrochem. Soc. 157 (2010) A8.
[22] H.-M. Cho, H.-C. Shin, in: G.R. Dahlin, K.E. Strom (Eds.), Lithium Batteries: Research, Technology and Applications, Nova Science, New York, 2010.
[23] H. Abe, K. Zaghib, K. Tatsumi, S. Higuchi, J. Power Sources 54 (1995) 236.
[24] Y.-M. Choi, S.-I. Pyun, Solid State Ionics 99 (1997) 173.
[25] D. Aurbach, M.D. Levi, E. Levi, H. Teller, B. Markovsky, G. Salitra, U. Heider, L. Heider, J. Electrochem. Soc. 145 (1998) 3024.
[26] W. Weppner, R.A. Huggins, J. Electrochem. Soc. 124 (1977) 1569.
[27] L.J. Fu, H. Liu, C. Li, Y.P. Wu, E. Rahm, R. Holze, H.Q. Wu, Solid State Sci. 8 (2006) 113.
[28] B. Kim, C. Kim, T.-G. Kim, D. Ahn, B. Park, J. Electrochem. Soc. 153 (2006) A1773.
[29] H. Zhao, J. Ren, X. He, J. Li, C. Jiang, C. Wan, Solid State Sciences 10 (2008) 612.
[30] P. Ghosh, S. Mahanty, R.N. Basu, Electrochim. Acta 54 (2009) 1654.
[31] M. Mancini, F. Nobili, S. Dsoke, F. D'Amico, R. Tossici, F. Croce, R. Marassi, J. Power Sources 190 (2009) 141.
[32] Y.S. Jung, A.S. Cavanagh, A.C. Dillon, M.D. Groner, S.M. George, S.-H. Lee, J. Electrochem. Soc. 157 (2010) A75.
[33] G.G. Amatucci, F. Badway, A. Du Pasquier, T. Zheng, J. Electrochem. Soc. 148 (2001) A930.
[34] I. Plitz, A. Dupasquier, F. Badway, J. Gural, N. Pereira, A. Gmitter, G.G. Amatucci, Appl. Phys. A 82 (2006) 615.
[35] Q. Qu, L. Li, S. Tian, W. Guo, Y. Wu, R. Holzeb, J. Power Sources 195 (2010) 2789.
[36] A. Du Pasquier, I. Plitz, J. Gural, F. Badway, G.G. Amatucci, J. Power Sources 136 (2004) 160.
[37] X. Hu, Z. Deng, J. Suo, Z. Pan, J. Power Sources 187 (2009) 635.